



ORIGINAL ARTICLE

The inhibition behavior of two pyrimidine-pyrazole derivatives against corrosion in hydrochloric solution: Experimental, surface analysis and in silico approach studies



Nadia Arrousse^{a,*}, R. Salim^{a,b}, Y. Kaddouri^c, Abdelkader zarrouk^e, D. Zahri^a, F. El Hajjaji^a, R. Touzani^c, M. Taleb^a, S. Jodeh^{d,*}

^a *Laboratory of Engineering, Electrochemistry, Modeling and Environment (LIEME), Faculty of Sciences, University Sidi Mohamed Ben Abdellah, Fez, Morocco*

^b *Laboratory of Separation Processes, Faculty of Science, University IbnTofail, Kenitra, Morocco*

^c *Laboratory of Applied Chemistry and Environment (LCAE), Faculty of Sciences, University Mohammed Premier Oujda, Morocco*

^d *Department of chemistry, An-Najah National University, P.O. Box 7, Nablus, Palestine*

^e *Laboratory of Materials, Nanotechnology and Environment, Departement of Chemistry, Faculty of Sciences, Mohammed V University, Rabat, Morocco*

Received 28 January 2020; accepted 24 April 2020

Available online 19 May 2020

KEYWORDS

Pyrimidine-pyrazole;
DFT;
EIS;
Mild steel;
In silico approach studies;
El Awady isotherm

Abstract Two pyrimidine-pyrazole derivatives have been investigated as corrosion inhibitors for mild steel in acidic medium using weight loss measurement, polarization curve and electrochemical impedance spectroscopy (EIS). The results obtained reveal that these compounds perform as corrosion inhibitors for mild steel in 1 M HCl. The values of inhibition efficiency calculated from three experimental techniques are reasonably in good agreement. The adsorption process of these compounds on surface of mild steel obeys to El Awady isotherm. Also, the adsorption process of inhibitors studied explaining by surface analysis (EDX). This work followed by in silico approach studies. Firstly, we used MarvinSketch.18 program in order to detect predominant form of inhibitors in electrolytic solution and then computed by Gaussian 09 based on the DFT method at B3LYP/6-31G (d, p). The results obtained theoretically are in good correlation with those obtained experimentally.

© 2020 The Author(s). Published by Elsevier B.V. on behalf of King Saud University. This is an open access article under the CC BY-NC-ND license (<http://creativecommons.org/licenses/by-nc-nd/4.0/>).

* Corresponding authors.

E-mail addresses: nadiaarrousse@gmail.com (N. Arrousse), el.hajjajifadoua25@gmail.com (F.E. Hajjaji), sjodeh@hotmail.com (S. Jodeh).
Peer review under responsibility of King Saud University.



1. Introduction

One of the most common problems in industries is the degradation of materials (Salim et al., 2017) in acidic medium by chemical reaction (Ismaili and Ouazzani, 2016). Therefore, several researches fight against this phenomenon of corrosion by action on the environment, through of using organic inhibitors (Banerjee and Chattopadhyaya, 2017; Rahmani et al., 2019). The protection of materials with using organic inhibitors is often associated to physical and/or chemical adsorption by transfer of the inhibitor electron on the surface of materials in order to form coordination or electrostatic bonds, or both (Banerjee and Chattopadhyaya, 2017). These properties depend on the nature of the inhibitors (heteroatoms, aromaticity...) (El Arrouji et al., 2015). The most smart inhibitors of corrosion in acidic medium are those compounds containing heteroatoms such as nitrogen, oxygen, sulphur and phosphorus which block the active sites and decrease the corrosion rate (Olayemi Abdulazeez et al., 2016).

The pyrimidine-pyrazole derivatives are nitrogen heterocycles widely used in medicine (Karrouchi et al., 2018). These compounds possess many biological activities (Kumar et al., 2014) such as antibacterial (El Hafi et al., 2018), anticonvulsive, antifungal, antiviral (Richards et al., 2019), antidiabetic and anticancer properties (Salim et al., 2019). Not only that, many researches have examined the inhibitory effect of these compounds on the corrosion of mild steel in acidic media and showed a high respects to the environment (Kumar et al., 2014; Walczak et al., 2018).

The aim of this work is to study the effect of two newly organic pyrimidine-pyrazole compounds on corrosion inhibition of mild steel in 1 M HCl medium using weight loss (direct method), also polarization curve and electrochemical impedance spectroscopy (indirect methods) Table 1. To improve the results obtained experimentally: we use MarvinSketch.18 program to detect the protonated forms of these compounds and be closer to the experience conditions. Therefore, the quantum chemical approach were computed using Gaussian 09 based on DFT B3LYP/6-31G (d,p) to calculate various quantum descriptors.

2. Experimental technical

2.1. Synthesis of DPP and PP

For the preparation of B, 2-aminopyrimidine-4,6-diol (5 g, 39 mmol) was stirring at 70 °C to solubilize it in 50 ml of acetonitrile, then we put the solution of (1H-pyrazol-1-yl) methanol (3.85 g, 39 mmol), the mixture was refluxed for 6 h,

Table 1 Inhibitors structures, names and abbreviations of the studied pyrimidine-pyrazole derivatives.

Abbreviation	Structure	IUPAC Name
DPP		2-(((2,3-dihydro-1H-pyrazol-1-yl)methyl)amino)pyrimidine-4,6-diol
PP		2-bis((1H-pyrazol-1-yl)methyl)amino)pyrimidine-4,6-diol

evaporated then filtered and washed with acetonitrile to obtain pink solid product. Same procedure to obtain C, but using 0.5 equivalent of 2-amino-6-methylpyrimidin-4-ol (5 g, 39 mmol) with (1H-pyrazol-1-yl) methanol (7.7 g, 78 mmol) which was stirred for 7 days under room temperature, filtered and washed with acetonitrile to obtain a pink solid product (Kaddouri et al., 2017). Fig. 1.

• DPP: 2-(((1H-pyrazol-1-yl) methyl) amino) pyrimidine-4,6-diol

The structure of the new organic dye was determined by spectroscopic methods: 1H NMR, and Infrared in order to get information about inhibitors structure.

Pink solid, Yield : 88%, Mp = > 250 °C, FTIR (KBr, cm⁻¹): 3372 (C-O), 2930 (C-H), 1750 (C = O), 1630 (C = N), 1562 (C-N), 1280 (C-C), 1030 (N-N), 915 (-C-H), 645 (=C-H), RMN 1H (DMSO, 500 MHz) δ ppm: 7,6 (d, 1H, CH (5)); 7,31 (d, 1H, CH (3)); 6,26 (dd, 1H, CH (4)); 6,11 (t, 1H, NH); 5,70 (s, 2H, CH₂); 4,85 (s, 1H, CH (pyrimidine)). Fig. 2.

• PP: 2-bis((1H-pyrazol-1-yl) methyl) amino) pyrimidine-4,6-diol

Pink solid, Yield: 94%, Mp = > 250 °C, FTIR (KBr, cm⁻¹): 3330 and 3260 (C-OH), 1670 (CH = CH), 1640 (C = N); 1475

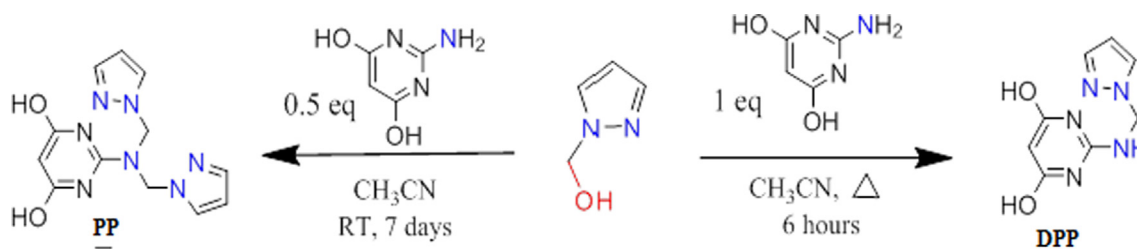


Fig. 1 General procedure for the preparation of DPP and PP.

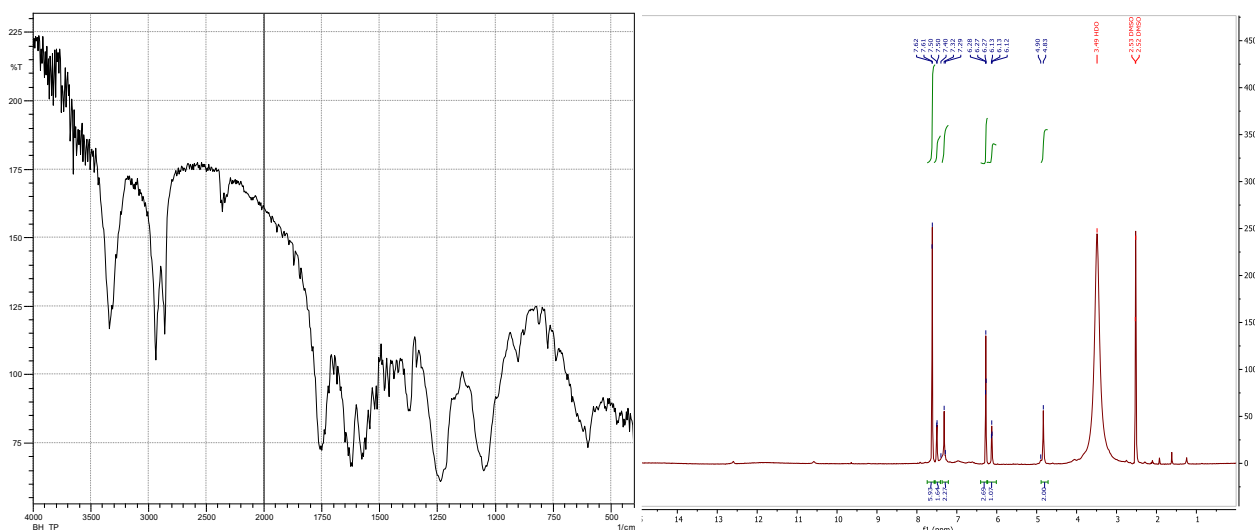


Fig. 2 The FTIR and ^1H NMR spectra of **DPP**: 2-(((1H-pyrazol-1-yl) methyl) amino) pyrimidine-4,6-diol.

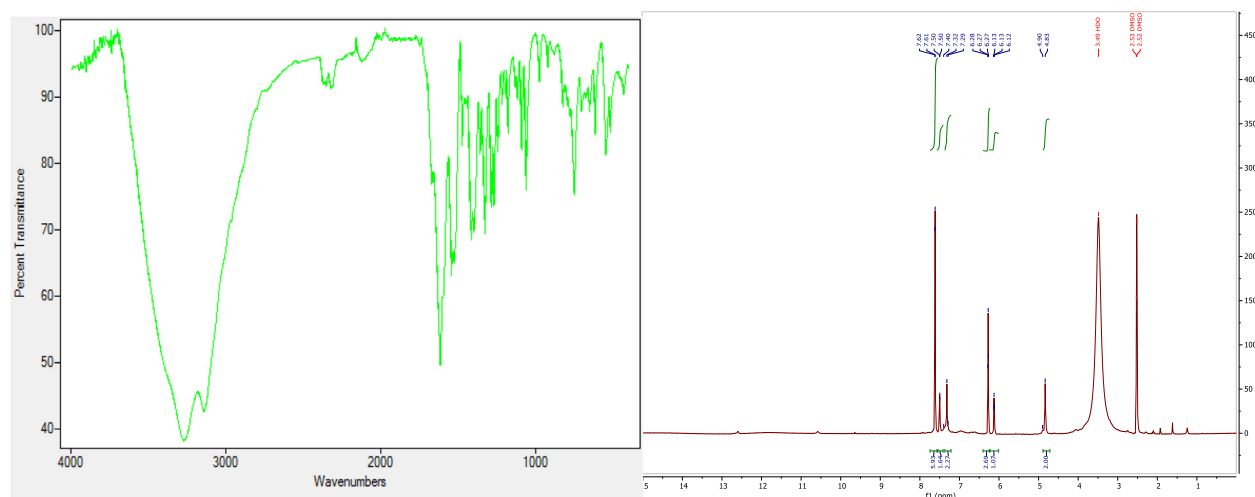


Fig. 3 The FTIR and ^1H NMR spectra of **PP**: 2-(bis((1H-pyrazol-1-yl) methyl) amino) pyrimidine-4,6-diol.

($-\text{CH}_2-$), 1365 (C-H), 1067 (C-C); RMN ^1H (DMSO, 500 MHz) δ ppm: 7.47 (s, 1H, OH); 7.29 (s, 1H, CH (4)); 6.09 (d, 1H, CH (3)); 5.76 (d, 1H, CH (5)); 4.80 (s, 2H, CH_2). **Fig. 3**.

2.2. Materials preparation

Mild steel undergoes before each trial a polishing of the surface on emery paper with different granulometry. Washed with distilled water to remove the mass impurities, degreasing by acetone and dry before start experiment to obtain true results. The hydrochloric acid 1 M prepared by dilution of analytical grade 37%. **Table 2**.

2.3. Gravimetric method

The mild steel is accurately weighted and immersed in 50 ml of hydrochloric acid 1 M without and with different concentrations of inhibitors. For the effect of concentration, the substrates immersed in the solution during 6 h at 298 K, and 2 h at temperature range 308–338 K in order to estimate their effect of temperature. When, the experience is finished the samples were taken out, washed with distilled water, dried and reweighed accurately. The inhibition efficiency (IE_{Grav} %) and corrosion rate (W_{corr}) was calculated according to the following equations (Mohamed Abdelahi et al., 2017):

Table 2 The material used in this work is mild steel with the following chemical composition.

Composition	Fe	C	Mn	Si	S	P	Al
Weight en %	99.21	0.21	0.05	0.38	0.05	0.09	0.01

$$IE_{\text{Grav}} \% = \frac{W_{\text{corr}} - W_{\text{corr}/\text{inh}}}{W_{\text{corr}}} * 100 \quad (1)$$

where W_{corr} and $W_{\text{corr}/\text{inh}}$ are the values of corrosion rates in the absence and the presence of inhibitors, respectively.

$$W_{\text{corr}} = \frac{\Delta m}{S * t} (\text{mg cm}^{-2} \text{h}^{-1}) \quad (2)$$

where $\Delta M(\text{mg})$ is the average weight loss, $S(\text{cm}^2)$ is the total area for substrate and $t(\text{h})$ is the immersion time in solution.

2.4. Electrochemical measurements

Electrochemical measurements realized by using a potentiostat Tacussel-Radiometer PGZ 100. The different electrochemical tests carried out by three-electrode glass cell. The mild steel used as the working electrode, Ag/AgCl electrode as the reference electrode and platinum as the counter electrode. Before all tests, the potential stabilized during 30 min, in order to get the open circuit potential and have a good electrochemical result. The anodic and cathodic polarization curves were recorded at an output rate of 1 mV/s and in order to get the EIS result, the applied frequency ranged from 100 KHz to 100mHz with 10 points per decade.

2.5. Surface morphology analysis

Among the great method for surface morphology analysis is the scanning electron microscopy. Therefore, in order to find available information about adsorption behavior of our tested inhibitors, the scanning electron microscopy (SEM) technical were used after an immersion during 6 h with and without DPP and PP inhibitors at 10^{-3}M . The material composition is obtained using energy dispersive X-ray (EDX) attached to the scanning electron microscopy with an acceleration voltage of 20 kV.

2.6. Quantum chemical approach

Recently, experimental researchers are convinced that the use of quantum chemical approach plays an important role in all

Table 3 Concentration effect of studied inhibitors in 1 M HCl obtained from weight loss measurements at 298 K.

Medium	Concentration (mol/L)	Corrosion rate (mg. $\text{cm}^{-2} \text{h}^{-1}$)	$IE_{\text{Grav}} \%$
HCl	1	0.6532	–
DPP	10^{-3}	0.1241	81
	10^{-4}	0.1661	75
	10^{-5}	0.3005	54
	10^{-6}	0.4246	35
PP	10^{-3}	0.0522	92
	10^{-4}	0.1110	83
	10^{-5}	0.1502	77
	10^{-6}	0.3723	43

areas of chemistry, the field of corrosion studies also can be used theoretical approach (Khaled, 2010). This approach was executed using MarvinSketch program in order to find the forms of inhibitors exist in experience conditions and Gaussian 09 program package using DFT/(B3LYP) with a basis set 6-31G (d,p) (El Assiri et al., 2019). In order to assimilate a correlation between theory and experimental studies as well as to detect the relation between inhibition efficiency and molecular properties estimated such as the highest occupied molecular orbital (HOMO), lowest unoccupied molecular properties and find the information at atomic scale by using Fukui indices calculations (Khaled, 2010).

3. Results and discussion

3.1. Gravimetric measurements

3.1.1. Effect of concentration

The value of corrosion rate of mild steel and inhibition efficiency at different concentrations of pyrimidine-pyrazole derivatives in acidic medium (1 M HCl) at 298 K obtained from weight loss method are given in Table 3. The gravimetric results indicate that the protective effect of inhibitors PP and DPP increases with concentration to attain 93% and 89% at 10^{-3}M , respectively. This performance reported to ability of a molecule to adsorb on the mild steel surface this compartment depends to the structure of inhibitors DPP and PP. Such

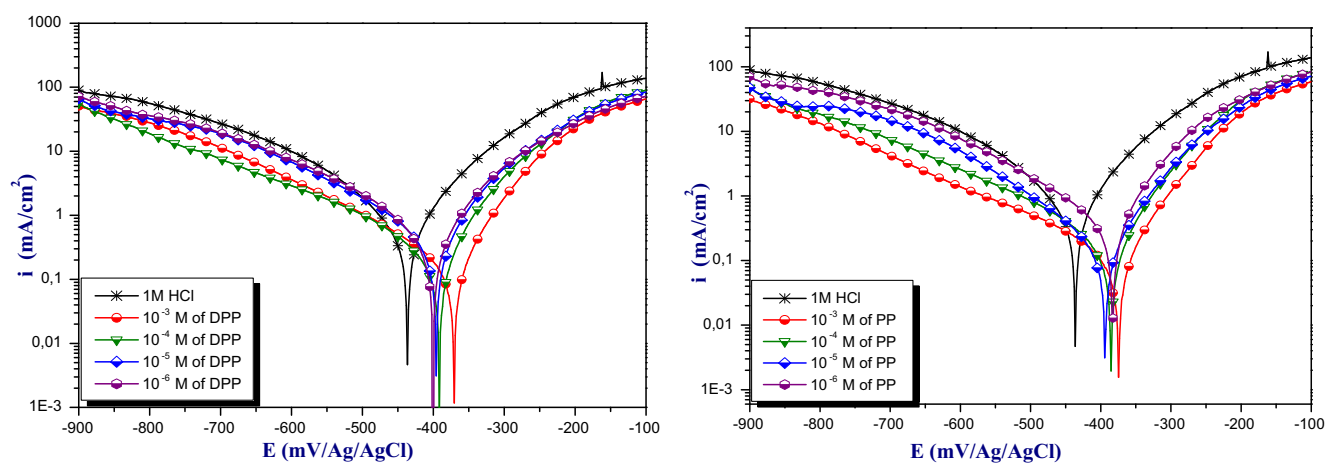


Fig. 4 Polarization curves for mild steel in the absence and presence of DPP and PP at various concentrations of inhibitors at 298 K in acidic medium.

Table 4 Kinetic parameters for mild steel in 1 M HCl containing different concentrations of inhibitors at 298 K.

Medium	Conc.M	$-E_{corr}mV/SCE$	$i_{corr}\mu A.cm^{-2}$	$-\beta_{cm}V.dec^{-1}$	$\beta_{am}V.dec^{-1}$	$IE_{PP}\%$
HCl	1	437	983	150	110	—
DPP	10^{-6}	401	672	170	102	32
	10^{-5}	396	468	165	88	52
	10^{-4}	392	279	161	72	72
	10^{-3}	370	189	155	66	81
PP	10^{-6}	383	578	160	75	40
	10^{-5}	393	221	141	80	76
	10^{-4}	385	172	158	73	83
	10^{-3}	375	82	152	66	92

as, nature of substitution in the inhibitor molecule (Ismaili and Ouazzani, 2016), presence of heteroatoms and delocalized π electrons in the aromatic ring of the pyrimidine-pyrazole derivatives and the vacant d-orbital of metal surface (Mohamed Abdelahi et al., 2017).

3.2. Potentiodynamic polarization measurements

3.2.1. Effect of concentration

Figure 4 showed the Polarization curves of mild steel in acidic medium obtained in the presence and absence of different con-

centrations of DPP and PP. All electrochemical parameters including I_{corr} , E_{corr} , Tafel slopes (β_c , β_a) and $IE\%$ were measured by extrapolation of Tafel curves are summarized in Table 4. The percentage of inhibition efficiency ($IE_{PP}\%$) values were measured using the following equation (Zarrouk et al., 2012):

$$IE_{PP}\% = \frac{i_{corr} - i'_{corr}}{i_{corr}} * 100 \quad (3)$$

where i_{corr} and i'_{corr} are the values of corrosion current densities without and with inhibitors, respectively.

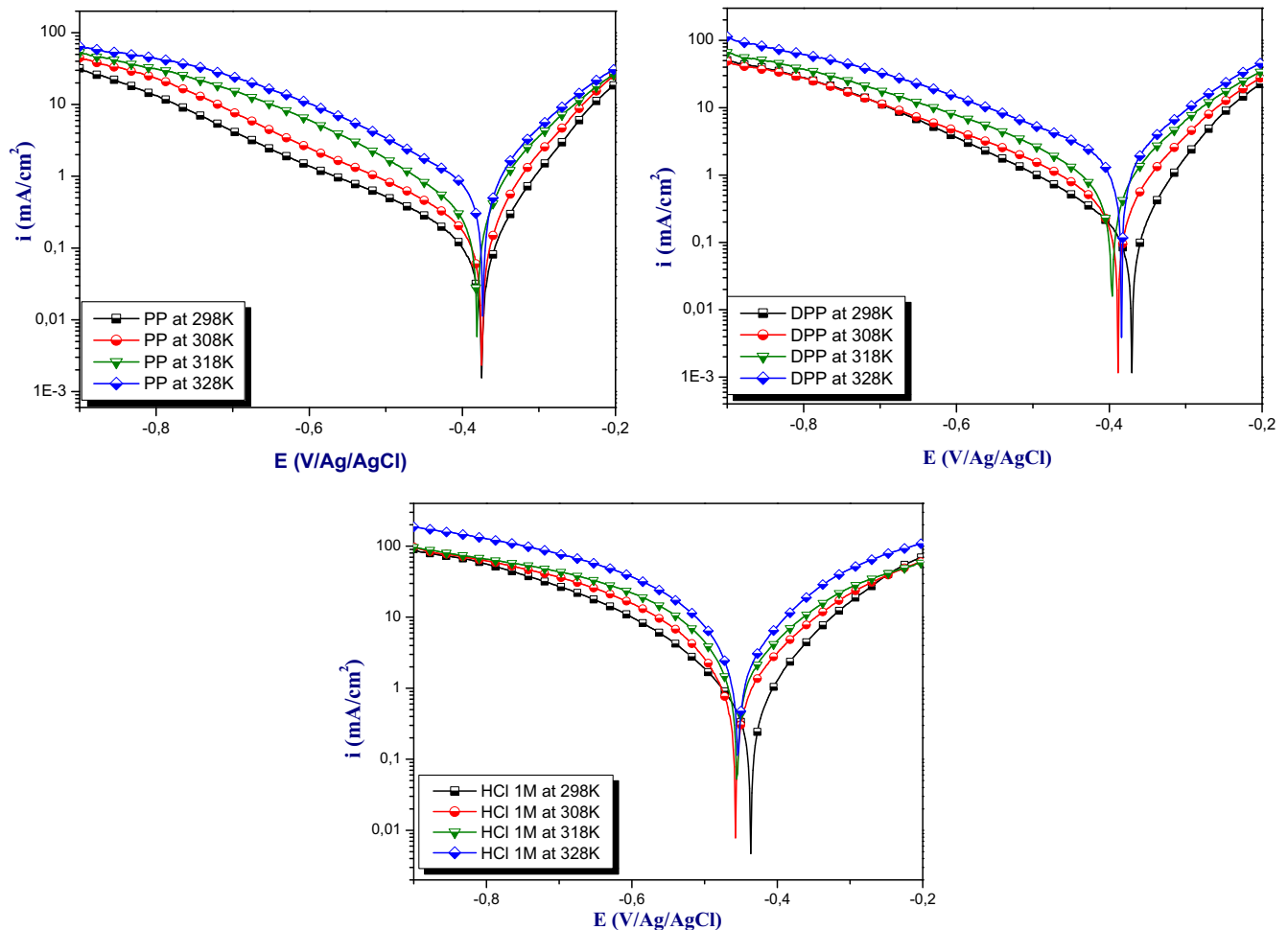
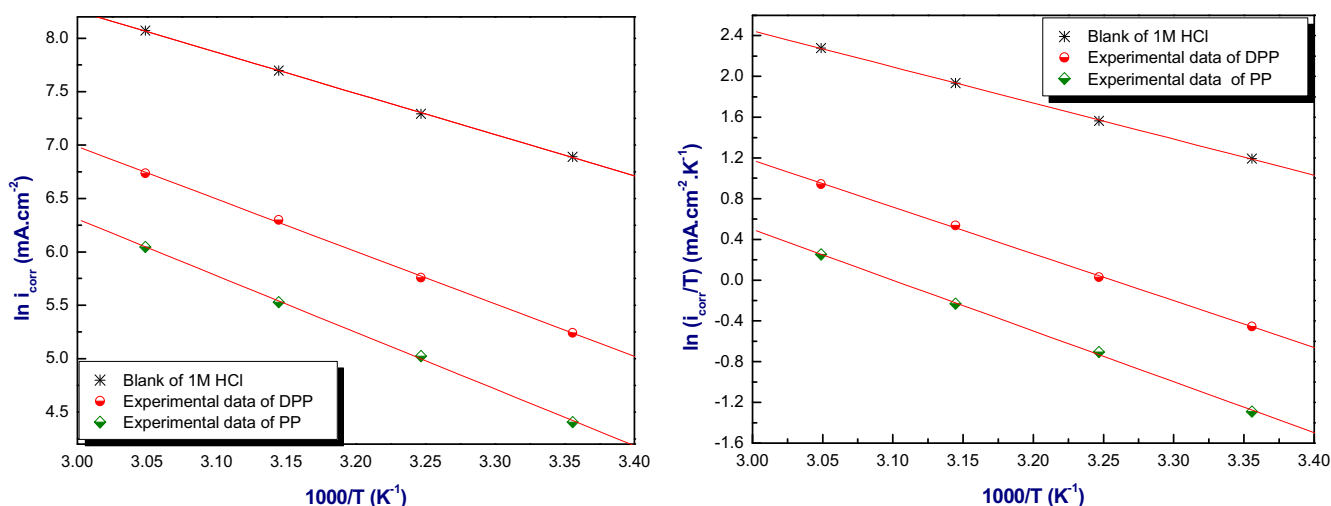


Fig. 5 Polarization curves in 1 M HCl obtained at $10^{-3}M$ of inhibitors at different temperature.

Table 5 Kinetics parameters of mild steel in 1 M HCl at different temperature.

Compounds	TemperatureK	$-E_{corr}mV/SCE$	$i_{corr}\mu A\ cm^{-2}$	$-\beta_c mVdec^{-1}$	$\beta_a mVdec^{-1}$	$IE_{PP}\%$
Blank	298	437	983	150	110	–
	308	456	1470	127	132	–
	318	455	2200	128	137	–
	328	454	3200	118	122	–
DPP	298	370	189	155	66	81
	308	389	317	157	81	78
	318	397	544	140	86	75
	328	384	841	101	67	74
PP	298	375	82	152	66	92
	308	374	152	161	67	90
	318	381	252	140	68	89
	328	373	422	107	63	87

**Fig. 6** Arrhenius plots of mild steel in 1 M HCl at optimal concentration of inhibitors.**Table 6** Thermodynamic parameters of the activation corrosion process of mild steel in HCL 1 M in the absence and presence of inhibitors at $10^{-3}M$.

Activation parameters	1 M HCl	DPP	PP
Ea (KJ/mol)	32,06	40,83	44,11
ΔH^* KJ/mol	29,47	38,23	41,51
ΔS^* (J/mol. K)	–88.9	–73.19	–69.0

The experimental result reveals that the current densities (i_{corr}) values decreases gradually with the increase in concentrations of two pyrimidine-pyrazole derivatives. Alongside, the inhibition effect increase with concentration of inhibitors and attains maximum values of 81% and 92% for DPP and PP, respectively at $10^{-3}M$. cathodicTafel slopes β_C , are roughly constant, it means that the inhibitors decreased the surface area for hydrogen evolution without influencing the reaction mechanism (Ech-chihbi et al., 2017). A survey literature shows that the displacement of E_{corr} compared to blank give information about the type of inhibitors tested: anodic

or cathodic type when the displacement of E_{corr} is superior to 85 mV with uninhibited solution, if not the inhibitor considered as mixed type (Beniken et al., 2018). In our case, the displacement in the E_{corr} value is less than 85 mV, this suggest that our inhibitors classified as mixed-type inhibitor with predominant anodic (Bouoidina et al., 2019).

3.2.2. Effect of temperature

Generally, the increase in temperature accelerates the phenomenon of corrosion because it decreases the domains of stability of the metals and accelerates the kinetics of reactions (El-Hajjaji et al., 2019). The polarization curves obtained without and with the optimum concentration $10^{-3}M$ of the studied inhibitors in 1 M hydrochloric acid solution at various temperatures were presented in Fig. 5. Nevertheless, the results regrouped in Table 5 showed a remarkable decrease in the densities of corrosion rate compared to the blank solution. In other side, this decreased is more pronounced in DPP inhibitors than PP inhibitor which confirming the adsorption behavior of PP inhibitor at the range temperature used.

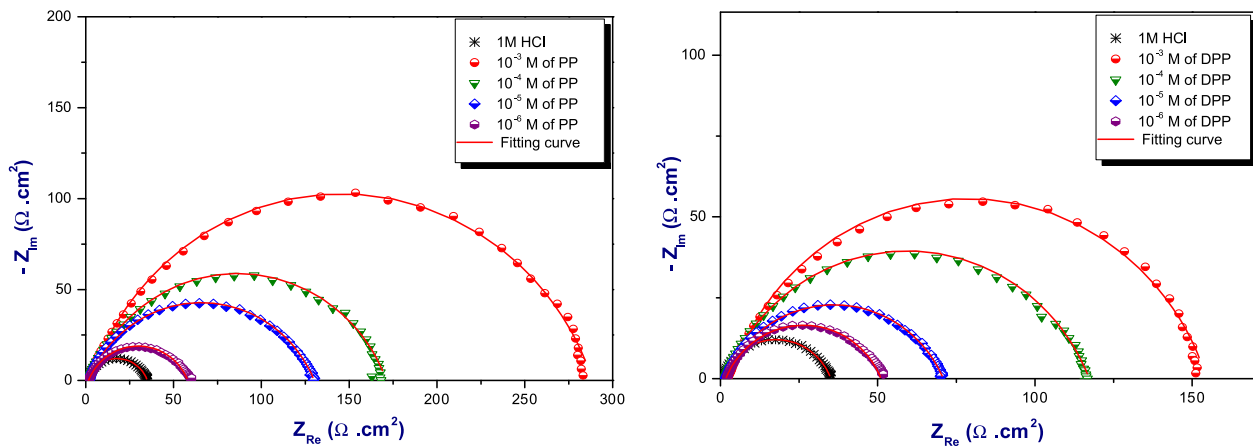


Fig. 7 The Nyquist plots diagrams for DPP and PP at 298 K in different concentrations.

3.2.3. Activation parameters

From this study, we can also calculate the thermodynamic activation parameters of the mild steel in acidic medium by using the Arrhenius equations (3) and (4) (EL Merimi et al., 2019):

$$i_{corr} = A e^{-\frac{E_a}{RT}} \quad (4)$$

$$i_{corr} = \frac{RT}{Nh} e^{\frac{\Delta S^\ddagger}{R}} e^{-\frac{\Delta H^\ddagger}{RT}} \quad (5)$$

where A is Arrhenius factor, R is the universal gas constant, N is Avogadro's number, T is the absolute temperature, h is Planck's constant ($h = 6.6252 \cdot 10^{-34}$ J.s), E_a , ΔH^\ddagger and ΔS^\ddagger are activation corrosion energy, the enthalpy and the entropy activation, respectively. Fig. 6.

Inspection of these results reveals that the values of ΔH^\ddagger for the dissolution reaction of mild steel in 1 M HCl in the presence of pyrimidine-pyrazole derivatives are more interesting to those obtained in the absence of inhibitors. In addition, the positive signs of the values of ΔH^\ddagger reflect the endothermic nature of the dissolution process of mild steel and suggesting that the dissolution of steel is slow in the presence of inhibitors (Tourabi et al., 2014) Table 6. The value of activation enthalpy is more important for inhibitor PP, which confirms the higher protection character compared to inhibitor DPP, and the difficulty of the dissolution of steel in the presence of this compound (Al-amiry et al., 2014). In other hand, the values of E_a in the presence of inhibitors are superior to control. Mean-

ing that our inhibitors adsorb on the surface of the steel by formation of electrostatic bonds (physical adsorption) according to the Radovici classifications (Rocca et al., 2019).

3.3. Electrochemical impedance spectroscopy (EIS)

The inhibition efficiency can also estimate by comparing the impedance values obtained in the presence and absence of inhibitors at different concentrations in acidic medium. The Nyquist plots for mild steel obtained with and without DPP and PP at 298 K are represent in Fig. 7. The inhibition efficiency in this case was calculated by the following equation:

$$IE_{imp}\% = [R_{ct} - R'_{ct}/R_{ct}] \times 100 \quad (6)$$

It can be seen from Fig. 7, the EIS diagrams are constituted of one-half loop which mean that ;the reaction of inhibitors DPP and PP on the working electrode surface were controlled by charge transfer process related to the heterogeneous and irregular surface (Zarrok et al., 2012). The parameters obtained from this measurement was illustrated in Table7.

From first observation, the data obtained from Table 7 show that inhibitor PP is more effective than DPP. Which explained by the inhibition efficiency reached in 10^{-3} M, 88% for inhibitor PP and 77%for inhibitor DPP. Also, it can be seen that the charge transfer resistance R_{ct} increase with the concentration of inhibitor. However, the double layer capacity C_{dl} values reduce explicated by adsorption of the inhibitor molecules on the surface of the metal and formation of a pro-

Table 7 Impedance parameters and inhibition efficiency of mild steel in 1 M HCl in the presence of inhibitors at various concentrations obtained at 298 K.

Medium	Conc (M)	$R_s(\Omega.cm^2)$	$R_{ct}(\Omega.cm^2)$	$Q(\mu F.S^{n-1})$	n_{dl}	$C_{dl}(\mu F.cm^{-2})$	$IE_{imp}\%$
HCl	1	1.12	34.7	315.0	0.770	121.0	–
DPP	10^{-6}	1.72	49.3	279.4	0.751	67.8	30
	10^{-5}	1.30	69.6	257.0	0.739	62.1	50
	10^{-4}	1.38	115.9	171.9	0.761	50.3	70
	10^{-3}	2.08	151.6	100.6	0.806	36.8	77
PP	10^{-6}	1.61	56.5	324.5	0.751	86.4	39
	10^{-5}	1.36	128.7	153.0	0.747	40.4	73
	10^{-4}	1.69	169.5	143.4	0.772	47.9	80
	10^{-3}	2.54	286.1	83.5	0.792	31.4	88

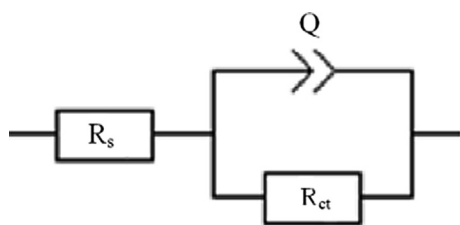


Fig. 8 Equivalent circuit model used in experimental impedance fit of M–steel in the presence and absence of inhibitors.

protective layer (El Hajjaji et al.). In addition, the factor of heterogeneity n_{dl} increase in inhibitor concentration related to the decrease of the surface heterogeneity and forming a protective film against the aggressive solution. It can be seen from the Nyquist plots that the shape of all semi-circle is not perfect. Therefore, the equivalent circuit presented in Fig. 8 modeled the capacitance double layer by element phase constant Q which gives us a best fitting for the Nyquist plots obtained (Beniken et al., 2018). The values of the inhibition efficiency obtained from EIS measurements showed the same trend as those obtained from the other techniques (Potentiodynamic polarization and weight loss methods).

3.4. Isotherm adsorption

The use of adsorption Isotherms is very important to determine the mechanism of adsorption of inhibitors to the surface of the metal (De Souza et al., 2014). For that, the experimental data of impedance was tested with various adsorption isotherms (Langmuir, Freundlich, El Awady, Frumkin, Flory-Huggins and Timken) Table 8. To do that, we used the following linear equations of each isotherm in order to find the model of isotherm explains the adsorption process of these inhibitors on the surface of mild steel (Beniken et al., 2018).

Where:

X: constitutes a measure of the value of adsorbed water molecules replaced by inhibitors molecules.

1/y: the number of water molecules removed by one molecule of inhibitor compound.

Z: This parameter explains the nature of mild steel/medium interfaces (homogeneous or heterogeneous).

A and d: represent the interaction factors among adsorbed molecules (repulsion or attraction force).

On the first, Langmuir's isotherm not verified despite the correlation coefficient very closed to unity since the second hypothesis of Langmuir isotherm not verified because the slope is superior to 1. On the other hand, the constant of adsorption has no significant for both Temkin and Freundlich isotherms. So, we can deduce that the adsorption process of these inhibitors follows El-Awady isotherm because is the most compatible when we compared the factor of regression obtained for the rest model traced and also, we can observe that their data were around the fitting curve compared to Frumkin and Flory-hugging isotherms Fig. 9. This model shows that one molecule of inhibitors can remove three molecules of water. In addition, the standard Gibbs energy (ΔG_{ads}^0) values near to -40 KJ mol^{-1} associated to chemical adsorption of inhibitors on the surface of mild steel by forming the coordination bonds (Banerjee and Chattopadhyaya, 2017). Table 9.

3.5. Surface analysis

The surface analysis studies of different species of mild steel in various cases with and without inhibitors after immersion during 6 h at 298 K in order to show the nature of atoms adsorbed on the surface of mild steel. SEM micrographs are shown in Fig. 10. The morphology of mild steel before immersion is smooth compared to the substrate after immersed in acidic solution, due to dissolution phenomenon. But, the presence of pyrazole derivatives inhibitors indicate the formation of a heterogeneous protecting film due to the formation of coordination bonds between inhibitors and the vacant orbital d of iron. Then, these results can be confirmed the adsorption phenomenon of inhibitors on the surface of material studied (Fig. 10 (C) (d)).

In order to characterize the chemical composition of material used in this work and the element adsorbed on the surface of mild steel after immersed in corrosive medium with and without inhibitors. The EDX method based on the analysis of X-rays emitted during electron-matter interaction. The results are shown in Fig. 11. The percentage atomic of different elements adsorbed on the surface of mild steel are illustrated in Table 10. From the values of percentage atomic of iron for mild steel immersed only in acidic solution and after addition of DPP and PP inhibitors. Because, the value of percentage of iron in DPP inhibitor more than PP inhibitor. This result shows that PP protects

Table 8 Linear forms of various isotherm equations.

Isotherms	Linear equations
Langmuir (Ezeibe et al., 2019)	$\frac{Cinh}{\theta} = \frac{1}{K} + Cinh$
El-Awady (Shariatinia and Ahmadi-Ashtiani, 2019)	$\log\left(\frac{\theta}{1-\theta}\right) = y \log K + y \log Cinh$
Flory-Huggins (Fathima et al., 2014)	$\text{Log}\left(\frac{\theta}{Cinh}\right) = \log K + x \log(1-\theta)$
Freundlich (El Hafi et al., 2018)	$\ln\theta = \ln K + z \ln Cinh$
Frumkin (El-Hajjaji et al., 2019)	$\ln Cinh \left(\frac{1-\theta}{\theta}\right) = -\ln K + 2d\theta$
Temkin (Ghazoui et al., 2017)	$\theta = -\frac{1}{2a} \ln K - \frac{1}{2a} \ln Cinh$

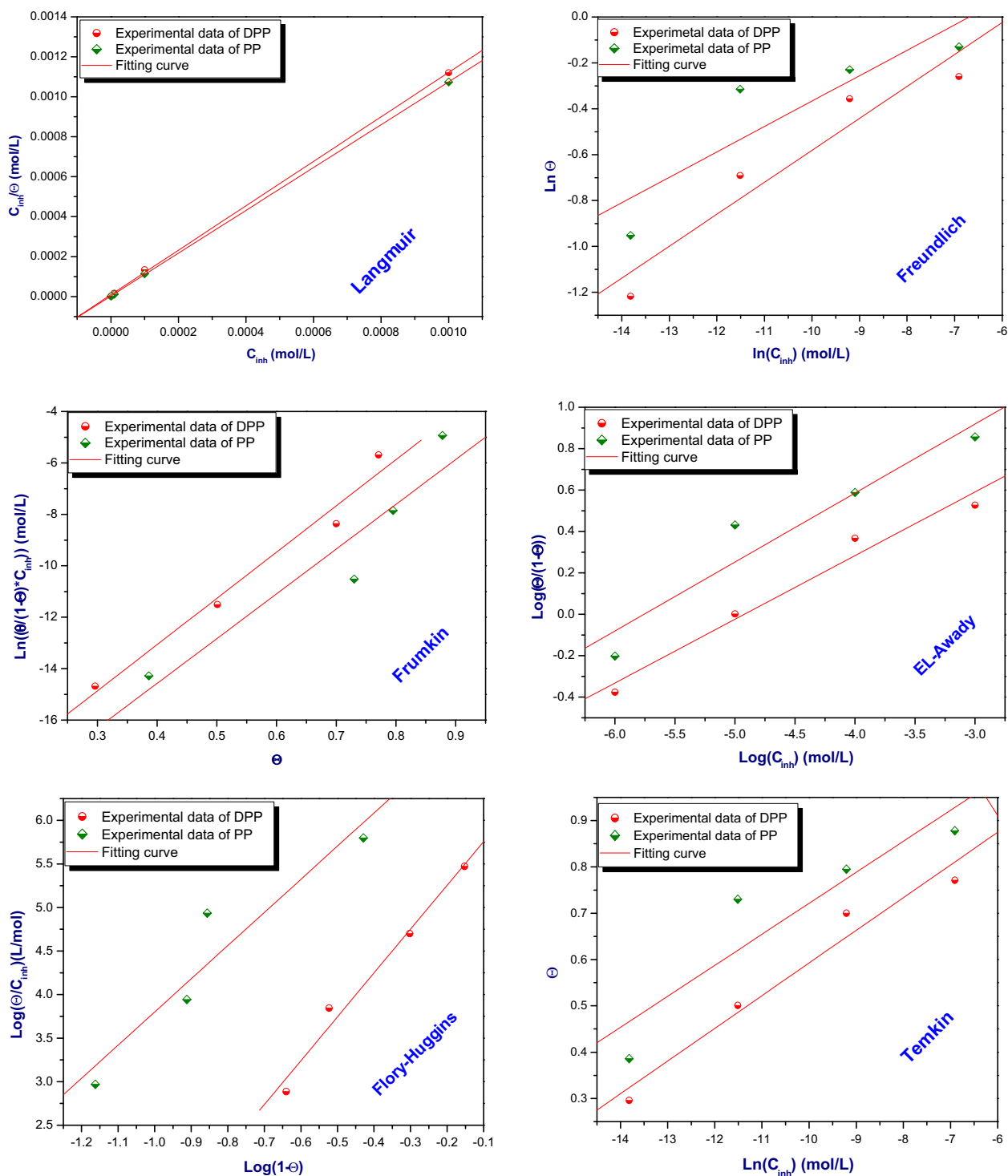


Fig. 9 Regrouped various isotherms models testing of DPP and PP on mild steel surface in hydrochloric acid medium at 298 K.

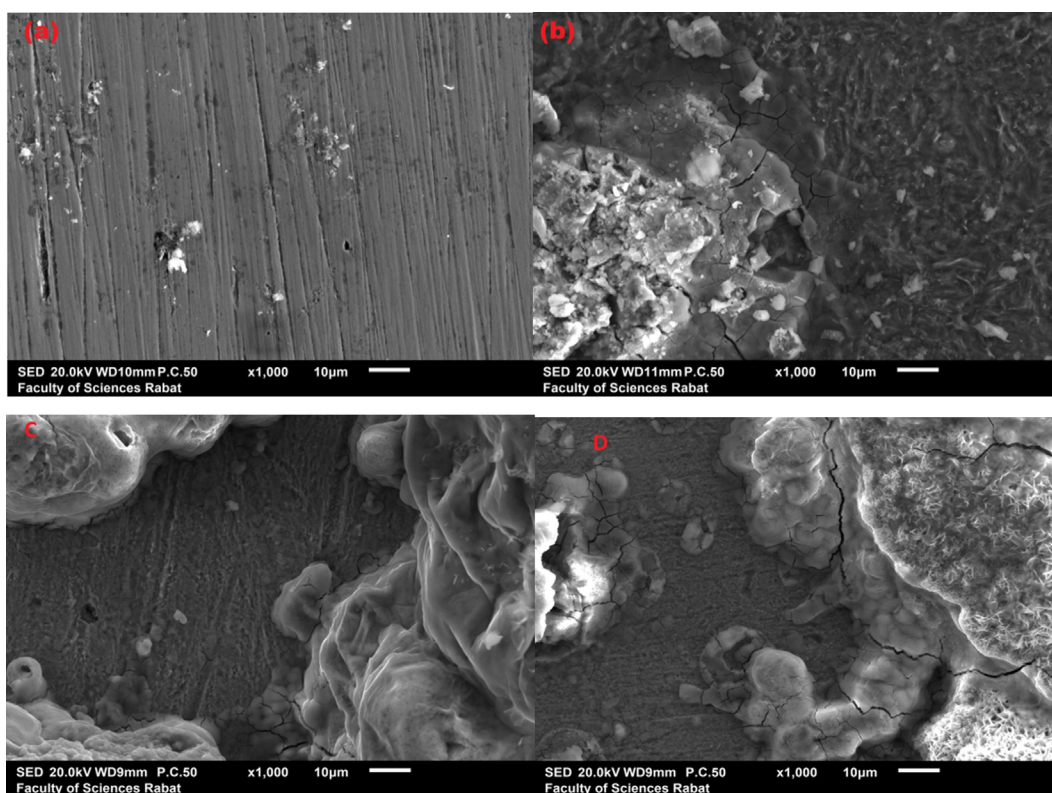
the mild steel against corrosion in molar hydrochloric acid solution more than DPP by adsorption of various heteroatom's such as: C, O and N. These results confirmed the order of efficiency obtained in experimental part by different methods (weight loss & electrochemical measurements) and theoretical study (DFT method).

3.6. *In silico* approach studies

Recently, experimental chemists are convinced that the use of quantum chemistry plays an important role in all areas of chemistry; the field of corrosion is no exception (Saady et al., 2019). The corrosion inhibition phenomenon was studied experimen-

Table 9 Parameters values from various K models of linearized isotherms equations for adsorption of DPP and PP inhibitors on the surface of mild steel in 1 M HCl at 298 K.

MMIsotherms	Inhibitors	R ²	Parameters	K	ΔG°_{ads} (Kj/mol)	
Langmuir	DPP	0,99	Slope	1,29	$1,34 \cdot 10^5$	-39,23
	PP	0,99	—	1,13	$1,94 \cdot 10^5$	-40,15
Freundlich	DPP	0,96	Z	0,14	2,25	-11,97
	PP	0,89	—	0,11	2,10	-11,77
El Awady	DPP	0,99	1/y	3,25	$8,38 \cdot 10^4$	-38,06
	PP	0,96	—	3,00	$1,60 \cdot 10^7$	-42,82
Frumkin	DPP	0,99	D	8,98	$1,6 \cdot 10^{-9}$	40,26
	PP	0,95	—	8,70	$4,44 \cdot 10^{-10}$	43,43
Florry-Huggins	DPP	0,99	X	5,03	$2,82 \cdot 10^{-6}$	21 ,72
	PP	0,95	—	3,81	$9,35 \cdot 10^{-8}$	30,17
Temkin	DPP	0,98	A	-7,09	1,06	-10 ,09
	PP	0,92	—	-7,47	1,05	-10 ,07

**Fig. 10** SEM micrographs of mild steel before immersion (a) after 6 h immersion in 1 M of HCl (b) after immersion in 10^{-3} M of DPP inhibitor (C) and of PP inhibitor (D).

tally in acidic medium. So, it is necessary to include the effect of solvent in the computations by searching the major protonated species in the electrolytic solution, in order to realize the better approach of experimental conditions (Teixeira et al., 2015). The MarvinSketch.18 program was used for the studied compounds. Therefore, the distribution of the protonated forms as a function of pH were presented in Fig. 12 with their predominant form obtained in 1 M HCl at PH close to zero.

It can be noticed from Table 11 that the molecule has eight species different, each one achieves a precise value. The analyses of these results show that the predominant form can be exist

in 1 M HCl solution for DPP compound have two protonated sites while PP molecules have three protonated sites at pH close to zero.

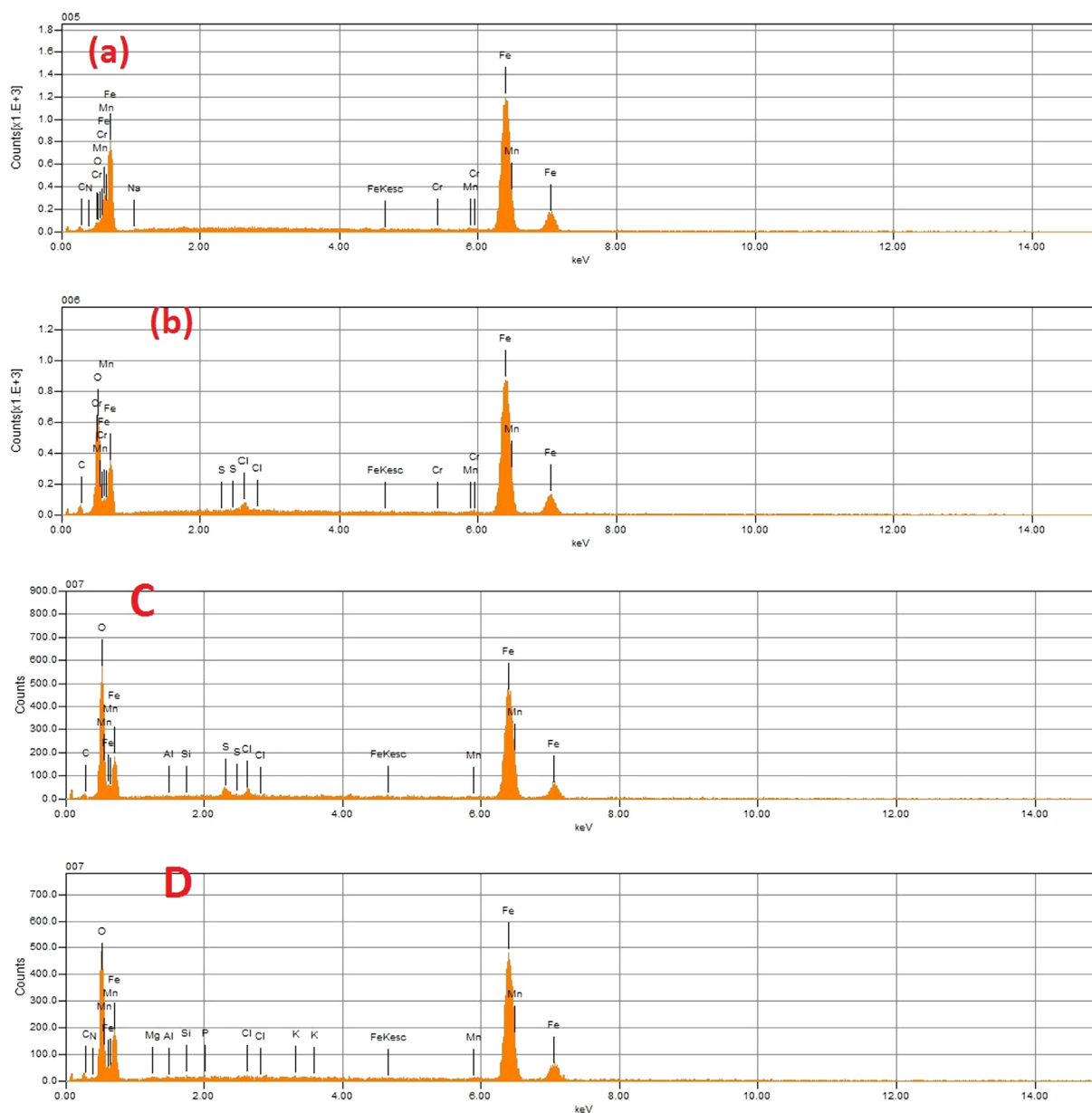
3.7. Quantum calculation

3.7.1. Global molecular reactivity of inhibitors compounds at protonated state

In order to obtain a good correlation between theoretical studies and experience. The computational studies of major species obtained by MarvinSketch was performed using

Table 10 Percentage atomic contents of elements obtained from EDX spectra.

Inhibitors	Fe	C	Cr	Mn	Cl	N	O
Mild steel	96.01	2.14	0.65	0.97	–	–	0.23
Mild steel in 1 M HCl	83.91	4.25	0.37	0.50	2.97	–	8.00
Mild steel in DPP	58.84	3.03	0.66	0.97	0.34	1.10	35.42
Mild steel in PP	50.34	4.70	0.30	0.69	0.18	8.38	35.41

**Fig. 11** EDX spectra of mild steel before immersion (a) after 6 h immersion in 1 M of HCl (b) after immersion in 10⁻³ M of DPP inhibitor C after immersion in 10⁻³ M of PP inhibitor D.

DFT, with B3LYP/6-31G (d,p) level implemented by Gaussian 09 program.

The interesting quantum chemical parameters using in this study for comparing the order of efficiency of these inhibitors regrouped in Table 12. These parameters extracted from the

result obtained by Gaussian such as: energy gap (ΔE), ionization potential (I), electron affinity (A), the absolute electronegativity (χ), global hardness (η), softness (σ) and the fraction of electrons transferred from the inhibitor molecule to the metal surface (ΔN) with $\eta_{Fe} = 0$ and $\chi = 7eV$ were calculated from

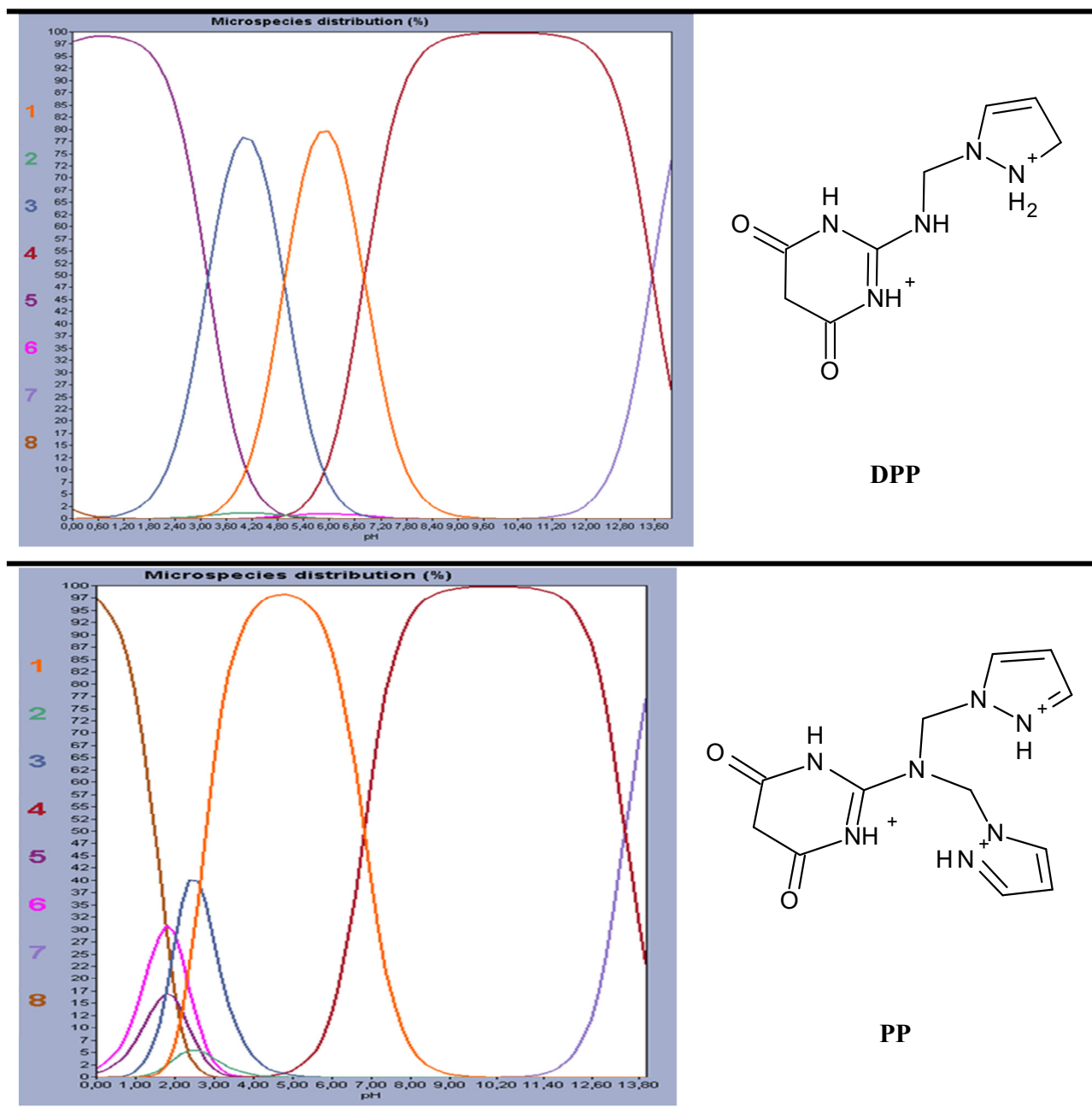


Fig. 12 Percentage of the observed species in terms of pH diagrams for DPP and PP compounds and the Predominate form obtained in 1 M HCl by MarvinSketch 18 program.

following relations and regrouped in Table 11 (Anusuya et al., 2015):

$$\Delta E = E_{LUMO} - E_{HOMO} \quad (7)$$

$$\chi = -\frac{1}{2}(E_{HOMO} + E_{LUMO}) \quad (8)$$

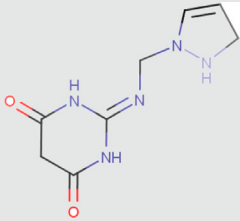
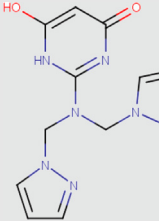
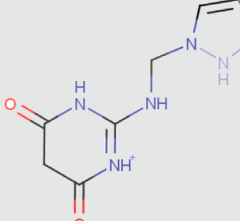
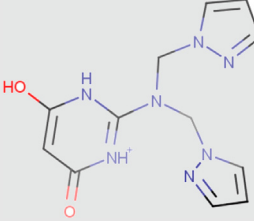
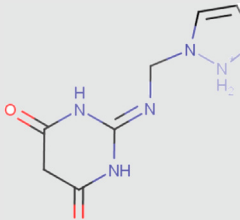
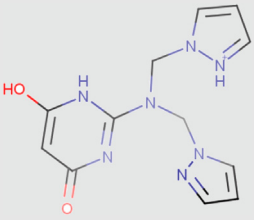
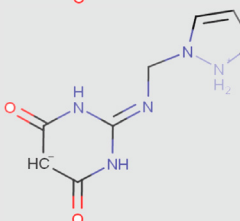
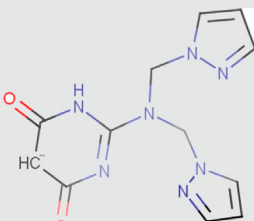
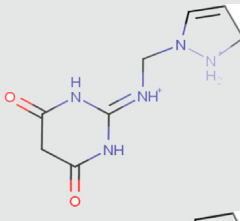
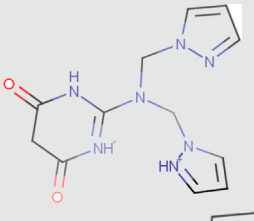
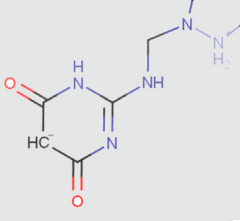
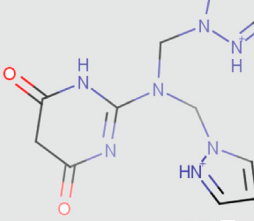
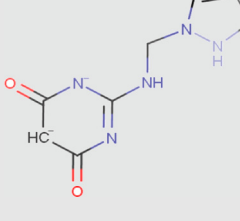
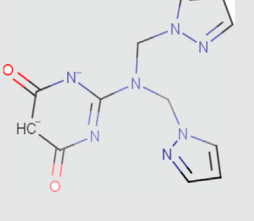
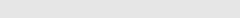
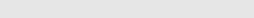
$$\eta = -\frac{1}{2}(E_{HOMO} - E_{LUMO}) \quad (9)$$

$$\sigma = \frac{1}{\eta} \quad (10)$$

$$\Delta N = \frac{\chi(Fe) - \chi(inh)}{2(\eta(Fe) + \eta(inh))} \quad (11)$$

Firstly, the lowest value of E_{LUMO} of PP shows the great capacity of the inhibitory molecule to accept electrons. In addition, it has the smallest Gap energy in comparison with the

Table 11 Shows the relation between the pH with the percentage of each species of DPP and PP compounds at pH = 0 obtained by MarvinSketch 18 program.

Species	DPP		PP	
	Structures	Percentage at pH = 0	structures	Percentage at pH = 0
1		0.00		0.00
2		0.00		0.00
3		0.07		0.01
4		0.00		0.00
5		97.96		0.88
6		0.00		1.61
7		0.00		0.00
8		1.96		97.49

(continued on next page)

Table 11 (continued)

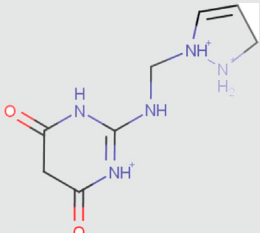
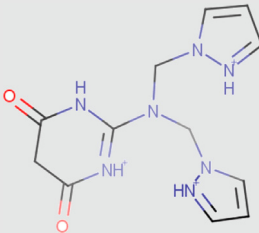
Species	DPP		PP	
	Structures	Percentage at pH = 0	structures	Percentage at pH = 0
				

Table 12 The principal theoretical parameters of DPP and PP in protonated state.

Inhibitors	DPP	PP
E_{HOMO} (eV)	-8.2936	-8.5228
E_{LUMO} (eV)	-5.9252	-6.1832
η	1.1842	1.1698
σ	0.8444	0.8548
ΔN	0.0462	0.1509
X	7.1094	7.3530
ΔE (eV)	2.3684	2.3396
$\mu(\text{D})$	14.9412	14.5190
Total energy (u.a)	-734.6990	-999.4399
IE (%) (EIS)	77	88

DPP inhibitor which would give a better reactivity to the PP molecule, because the excitation energy from the last orbital occupied will be low (Pang et al., 2012). Also, in the field of corrosion, the dipole moment as an indicator for reactivity, does not present the reasonable trend with the effectiveness of inhibitors. Indeed, according to some authors, it was reported that the dipole moment increases with increasing of inhibition efficiency. However, it's shown an opposite trend in other studies. In our case, it turns out that the dipole moment does not correlate with the inhibitory efficiency (Khaled, 2010). On the other hand, it can be clear that the PP inhibitor have a less value of hardness and high value of softness than DPP inhibitor which goes with the inhibition obtained experimentally. In our study $\Delta N < 3,6$ so according to Lukovist's study it reflects the increases in electron-donating ability to the metal surface this can be decreases the corrosion rate (Ben Hmamou et al., 2013). Generally, the electronegativity parameter gives knowledge about the capacity of molecule inhibitor to attract electrons to itself. In our case, PP inhibitor show us a high capacity to attract electrons to itself which confirm the adsorption of this compound compared to DPP molecule (Zarrouk et al., 2014). Finally, it can be concluded that the quantum chemical descriptors show a good correlation with experimental results.

The table Fig. 13 indicate that the HOMO and LUMO electron density of studied inhibitors DPP and PP focused around the pyrimidine and pyrazole ring. Indicating the capacity of these inhibitors to send and accept electrons and that the adsorption phenomenon is likely to occur on reactive sites distributed along the molecule inhibitors (Zarrok et al., 2012).

3.7.2. Local molecular reactivity of inhibitors compounds in protonated state

Fukui indices can provide valuable information on preferential sites for electrophilic (F_k^+ high) and/or nucleophilic (F_k^- high) attack (Al Mamari et al., 2016).

To identify sites favourable to nucleophilic and/or electrophilic attacks of these inhibitors compound. We carried out a calculation of the descriptors of the selectivity. For this, we opted for the Fukui indices (F_k^+ , F_k^- and F_k^0) calculated from the natural populations NPA of atoms while taking into account the effect of solvent for major species at pH = 0 according to the following Fukui equations (Saady et al., 2019):

$$F_k^+ = P_k(N + 1) - P_k(N) \quad (12)$$

$$F_k^- = P_k(N) - P_k(N-1) \quad (13)$$

$$F_k^0 = P_k(N + 1) - P_k(N-1) \quad (14)$$

From the calculated Fukui indices Table 13, we can say that the inhibitors studied have various sites for attacks in spite of protonated two sites (N11, N3) from DPP inhibitor and three sites from PP inhibitor (N16, N3, N11). They have also other sites capable to send and accept electrons such as (C6, O15) from B and (C6, O20) these reactive sites appear on the pyrimidine ring from these inhibitors and reflect their great inhibitory capacity (Abdel-Rehim et al., 2010).

4. Conclusion

The comparative study obtained for PP and DPP show a high inhibition performance of PP inhibitor (88%) against corrosion of mild steel in hydrochloric acid solution compared to DPP inhibitor (77%). These results were confirmed by different techniques experimentally. This behavior reflected to the existence of two pyrazole rings which increase the possibility to create more coordination bonds. Moreover, the both studied compounds shows that acted as a mixed type according to Tafel polarization curves results. In addition, it can be concluded from the adsorption isotherm analysis that the tested compounds obeyed to El Awady isotherm and that each molecule can replace three water molecules confirming therefore their strong adsorption onto the steel surface. These results were confirmed in the Insilco study showing that PP inhibitor at pH = 0 (pH of electrolyte solution) have a triprotonated form which is more than DPP inhibitor (diprotonated form).

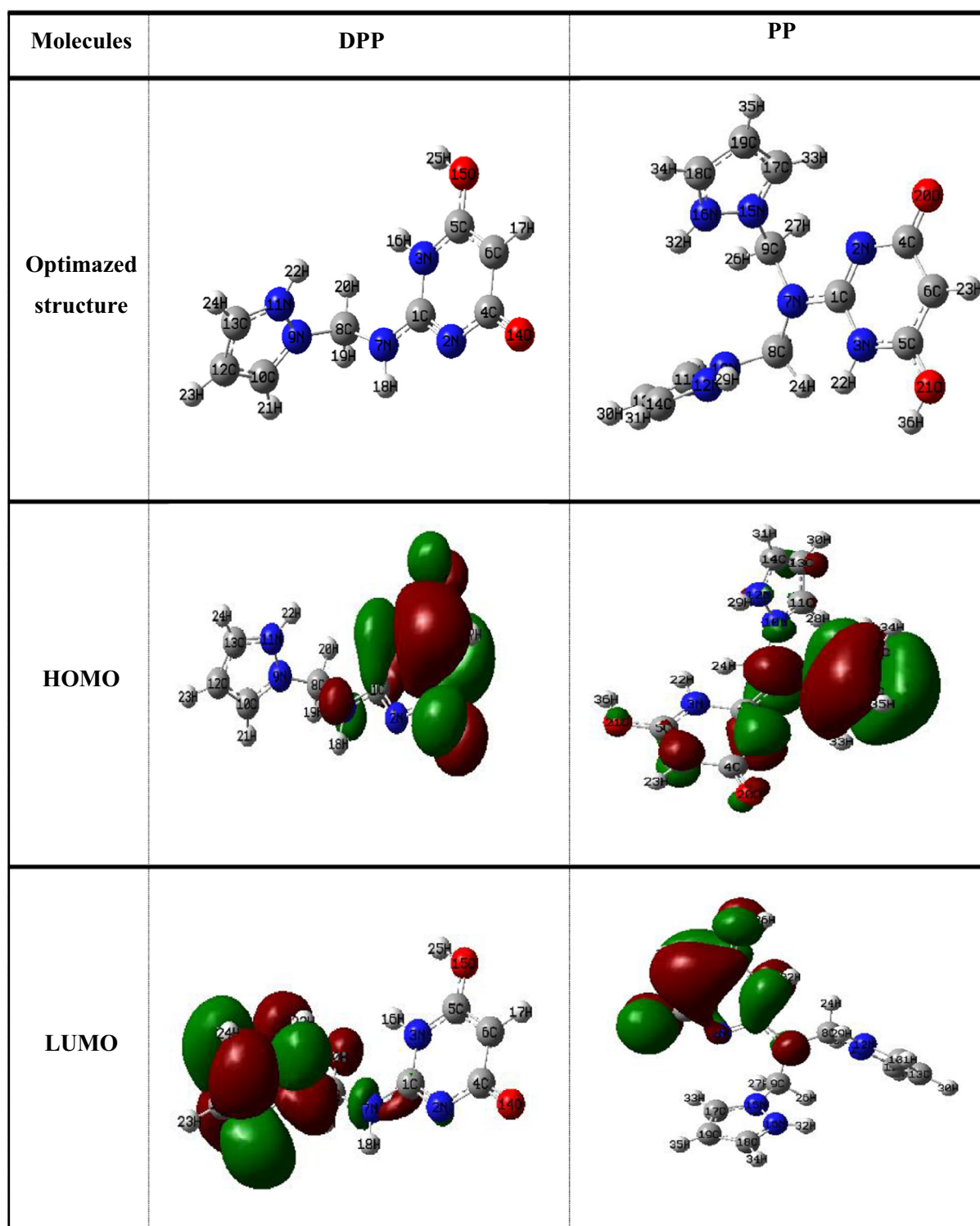


Fig. 13 The geometry optimization, HOMO and the LUMO distributions of the studied compounds obtained by B3LYP/6-31G (d,p) level at protonated state in aqueous phase.

Table 13 The natural populations and Fukui functions of the studied inhibitors computed at B3LYP/6-31G in protonated state.

Inhibitors	ATOMS	P(N)	P (N + 1)	P (N-1)	F ⁺ _k	F ⁻ _k	F ⁰ _k
DPP	N2	7.5697	7.6104	7.5087	0.0406	0.0610	0.0508
	N3	7.5721	7.6382	7.5039	0.0661	0.0681	0.0671
	C5	5.3361	5.4145	5.3438	0.0783	-0.0076	0.0353
	C6	6.1290	6.4745	5.8395	0.3454	0.2895	0.3175
	N7	7.6116	7.6502	7.4860	0.0385	0.1256	0.0820
	O14	8.4810	8.6949	8.3967	0.2139	0.0842	0.1490
	O15	8.5895	8.6667	8.5264	0.0771	0.0631	0.0701
PP	C1	5.3151	5.3354	5.3104	0.0203	0.0046	0.0125
	N2	7.5757	7.6104	7.5478	0.0346	0.0279	0.0313
	N3	7.5687	7.6296	7.5084	0.0609	0.0602	0.0605
	C6	6.1226	6.4604	5.8744	0.3377	0.2482	0.2930
	N7	7.4641	7.4924	7.3781	0.0282	0.0860	0.0571
	O20	8.4513	8.6774	8.3596	0.2260	0.0917	0.1588
	O21	8.5834	8.6619	8.5321	0.0784	0.0513	0.0649

Furthermore, the quantum chemical calculation parameters obtained are in good correlation with experimental result except the dipole moment which is goes in the opposite trend.

Declaration of Competing Interest

The authors declare that they have no known competing financial interests or personal relationships that could have appeared to influence the work reported in this paper.

References

- Abdel-Rehim, S., Khaled, F., Al-Mobarak, N., 2010. Corrosion inhibition of iron in hydrochloric acid using pyrazole. *Arab. J. Chem* 4, 333–337.
- Al Mamari, K., Elmsellem, H., Sebbar, N., Elyoussfi, A., Steli, H., Ellouz, M., Ouzidan, Y., Nadeem, A., Essassi, E.M., El-Hajjaji, F., 2016. Electrochemical and theoretical quantum approaches on the inhibition of Electrochemical and theoretical quantum approaches on the inhibition of mild steel corrosion in HCl using synthesized benzothiazine compound. *JMES* 7 (9), 3286–3299.
- Al-amiery, A., Kadhum, A., Kadhim, A., Mohamad, B., How, K., Junaedi, S., 2014. Inhibition of Mild Steel Corrosion in Sulfuric Acid Solution by New Schiff Base. *Materials* 7 (2), 787–804.
- Anusuya, N., Sounthari, P., Saranya, J., Parameswari, K., Chitra, S., 2015. Quantum Chemical Study on the Corrosion Inhibition Property of Some Heterocyclic Azole Derivatives. *Orient. J. Chem.* 31, 741–1750.
- Banerjee, S., Chattopadhyaya, M.C., 2017. Adsorption characteristics for the removal of a toxic dye, tartrazine from aqueous solutions by a low cost agricultural by-product. *Arab. J. Chem* 10, S1629–S1638.
- Ben Hmamou, D., Salghi, R., Zarrouk, A., Zarrok, H., Hammouti, B., 2013. Electrochemical and Gravimetric Evaluation of 7-methyl-2-phenylimidazo [1, 2- α] pyridine of Carbon Steel Corrosion in Phosphoric Acid Solution. *Int. J. Electrochem. Sci.* 8, 11526–11545.
- Beniken, M., Driouch, M., Sfaira, M., Hammouti, B., Ben Touhami, M., 2018. Kinetic – Thermodynamic Properties of a Polyacrylamide on Corrosion Inhibition for C-Steel in 1.0 M HCl Medium : Part 2. *J. Bio- Tribo-Corrosion* 4, 34.
- Beniken, M., Driouch, M., Sfaira, M., Hammouti, B., Ben Touhami, M., 2018. Anticorrosion Activity of a Polyacrylamide with High Molecular Weight on C-Steel in Acidic Media : Part 1. *J. Bio-Tribo-Corrosion* 38, 1–14.
- Bouoidina, A., El-hajjaji, F., Emran, Kh., Belghiti, M., Elaloui, A., Elmouky, A., Taleb, M., Abdellaoui, A., Abdellaoui, A., Ham-
- mouti, Obot, I.B., 2019. Towards Understanding the Anticorrosive Mechanism of Novel Surfactant Based on Mentha pulegium Oil as Eco-friendly Bio-source of Mild Steel in Acid Medium: a Combined DFT and Molecular Dynamics Investigation. *Chem. Res. Chinese Univ* 35 (1), 85–100.
- De Souza, F.S., Gonçalves, R.S., Spinelli, A., 2014. Assessment of Caffeine Adsorption onto Mild Steel Surface as an Eco-Friendly Corrosion Inhibitor. *J. Braz. Chem* 25 (1), 81–90.
- Ech-chihbi, E., Belghiti, M.E., Salim, R., Oudda, H., Taleb, M., Benchat, N., Hammouti, B., El-Hajjaji, F., 2017. Experimental and computational studies on the inhibition performance of the organic compound ‘2-phenylimidazo [1,2- α]pyrimidine-3-carbaldehyde’ against the corrosion of carbon steel. *Surf. Interfaces* 9, 1–29.
- El Arrouji, S., Alaoui, K.I., Zerrouki, A., Kadiri, S.E.L., Touzani, R., Rais, Z., Baba, M.F., Taleb, M., Chetouani, A., Aouniti, A., 2015. The Influence of Some Pyrazole Derivatives on The Corrosion Behaviour of Mild Steel in 1M HCl Solution. *JMES* 7 (1), 299–309.
- El Assiri, E., Driouch, M., Bensouda, Z., Beniken, M., Elhaloui, A., Sfaira, M., Saffaj, T., 2019. Analytical & Relationship between Corrosion Inhibition Efficiency and Derivatives on C-steel Surface. *Anal. Bioanal. Electrochem* 11 (3), 373–395.
- El Hafı, M., Ezzanad, A., Boulhaoua, M., El Ouasif, L., Saadouni, M., El Aoufir, Y., Ramli, Y., Zarrouk, A., Oudda, H., Essassi, E.M., 2018. Corrosion Inhibition Effect of Novel Pyrazolo [3,4-d] pyrimidine Derivative on Mild Steel in 1 M HCl Medium: Experimental and Theoretical Approach. *J. Mater. Environ. Sci* 9 (4), 1234–1246.
- El Hajjaji, Fadoua, Abridgach, Farid, Hamed, Othman, Hasan, Abdelfatah, Taleb, Mustapha, Jodeh, Shehdeh, Rodríguez-Castellón, Enrique, Martínez de Yuso, María, Algarra, Manuel, Hajjaji et al., Corrosion Resistance of Mild Steel Coated with Organic Material Containing Pyrazol Moiety. *Coatings* 8 (10), 330. <https://doi.org/10.3390/coatings8100330>.
- EL Merimi, Y., Ouadi, R., Benkaddour, H., Lgaz, M., Messali, F., Jeffali, Hammouti, B., 2019. Improving corrosion inhibition potentials using two triazole derivatives for mild steel in acidic medium: Experimental and theoretical studies. *Mater. Today: Proc.* 13, 920–930.
- El-Hajjaji, F., Merimi, I., Messali, M., Obaid, R.J., Salim, R., Taleb, M., Hammouti, B., 2019. Experimental and quantum studies of newly synthesized pyridazinium derivatives on mild steel in hydrochloric acid medium. *Mater. Today: Proc.* 13, 822–831.
- El-Hajjaji, F., Messali, M., Martínez de Yuso, M.V., Rodríguez-Castellón, E., Almutairi, S., Bandoz, Teresa J., Algarra, M., 2019. Effect of 1-(3-phenoxypropyl) pyridazin-1-ium bromide on steel corrosion inhibition in acidic medium. *J. Colloid Interface Sci.* 541, 418–424.

- Ezeibe, A., Nleonu, E., Ahumonye, A., 2019. Thermodynamics Study of Inhibitory Action of Lignin Extract from *Gmelina arborea* on the corrosion of mild steel in dilute Hydrochloric Acid. *International Journal of Scientific Engineering and Research* 7 (2), 133–136.
- Fathima, A., Abdul, S., Sethumanickam, S., 2014. Corrosion inhibition, adsorption and thermodynamic properties of poly (vinyl alcohol-cysteine) in molar HCl. *Arab. J. Chem* 10 (2), S3358–S3366.
- Ghazoui, A., Benchat, N., El-Hajjaji, F., Taleb, M., Rais, Z., Saddik, R., Elaataoui, A., Hammouti, B., 2017. The Study Of The Effect Of Ethyl (6-Methyl-3-Oxopyridazin-2-Yl) Acetate On Mild Steel Corrosion In 1M HCl. *J. Alloys Compounds* 693, 510–517.
- K. A. Ismaili, F. Ouazzani, Y. kandri rodi, A. M. Azaroual, Z. Rais, M. Filali Baba, M. Taleb, A. Chetouani, A. Aouniti, B. Hammouti (2016) "Effect of some Benzimidazolone compounds on C38 steel corrosion in hydrochloric acid solution" *JMES*, 7(1): 244-258.
- Y. Kaddouri, A. Takfaoui, R. El Ati, F. Abrigach, M. Lamsayah and R. Touzani, J. MAR (2017) "Synthesis of four new tridentate pyrazolic ligands", *chim. Heterocycl*, 16(1):100-104.
- Karrouchi, K., Radi, S., Ramli, Y., Taoufik, J., Mabkhot, Y., Al-azari, F., Ansar, M., 2018. Synthesis and Pharmacological Activities of Pyrazole Derivatives : A Review. *Molecules* 23 (1), 134.
- Khaled, K.F., 2010. Corrosion control of copper in nitric acid solutions using some amino acids – A combined experimental and theoretical study. *Corros. Sci.* 52, 3225–3234.
- Kumar, R., Arora, J., Ruhil, S., Phougat, N., Chhillar, A.K., Prasad, A.K., 2014. Synthesis and Antimicrobial Studies of Pyrimidine Pyrazole Heterocycles. *Advances in Chemistry* 2014, 1–12.
- Mohamed Abdelahi, M.M., Elmsellem, H., Benchidmi, M., Sebbar, N. K., Belghiti, M.A., El Ouasif, L., Jilal, A.E., Kadmi, Y., Essassi, E.M., 2017. A DFT and Molecular Dynamics Study on Inhibitory Action of indazole Derivative on Corrosion of Mild Steel. *JMES* 8 (5), 1860–1876.
- Olayemi Abdulazeez, M., Kolawole Oyebamiji, A., Semire, B., 2016. Dft and qsar study of corrosion derivatives with heteroatom on. *Leban. Sci. J* 17 (2), 217–232.
- Pang, X., Guo, W., Li, W., Xie, J., Hou, B., 2012. Electrochemical, quantum chemical and SEM investigation of the inhibiting effect and mechanism of cipro-floxacin, norfloxacin and ofloxacin on the corrosion for mild steel in hydrochloric acid. *Sci. China Ser* 51 (10), 928–936.
- Rahmani, H., Alaoui, K.I., Emran, K.M., El Hallaoui, A., Taleb, M., El Hajji, S., Labriti, B., Ech-chihbi, E., Hammouti, B., El-Hajjaji, F., 2019. Experimental and DFT Investigation on the Corrosion Inhibition of Mild Steel by 1, 2, 3- triazole Regioisomers in 1M hydrochloric Acid Solution. *Int. J. Electrochem. Sci.* 14, 985–998.
- Richards, C.A.J., McMurray, H.N., Williams, G., 2019. Smart-release inhibition of corrosion driven organic coating failure on zinc by cationic benzotriazole based pigments. *Corros. Sci.* 154, 101–110.
- Rocca, E., Faiz, H., Dillmann, P., Neff, D., Mirambet, F., 2019. Electrochemical behavior of thick rust layers on steel artefact: Mechanism of corrosion inhibition. *Electrochim. Acta* 316, 219–227.
- Saad, A., El-Hajjaji, F., Taleb, M., Ismaili Alaoui, K., El Biache, A., Mahfoud, A., Alhouari, G., Hammouti, B., Chauhan, D.S., Quraishi, M.A., 2019. Experimental and theoretical tools for corrosion inhibition study of mild steel in aqueous hydrochloric acid solution by new Indanones derivatives. *Mater. Discover* 12, 30–42.
- Salim, R., Elaataoui, A., Benchat, N., Ech-chihbi, E., Rais, Z., Oudda, H., El Hajjaji, F., ElAoufir, Y., Taleb, M., 2017. Corrosion behavior of a smart inhibitor in hydrochloric Acid molar: Experimental and theoretical studies. *JMES* 8 (10), 3747–3758.
- Salim, R., Ech-chihbi, E., Oudda, H., El Hajjaji, F., Taleb, M., Jodeh, S., 2019. A review on the assessment of imidazole [1,2-a] pyridines as corrosion inhibitor of metals. *J. Bio. Tribo. Corros.* 13, 5–11.
- Shariatnia, Z., Ahmadi-Ashtiani, A., 2019. Corrosion inhibition efficiency of some phosphoramidate derivatives: DFT computations and MD simulations. *Molecular Liquids* 298, 111–409.
- D.A. Teixeira, M.A. G. Valente, Jr. Assis, V. Benedetti, G. T. Feliciano, S. C. da Silva and C. S. Fugivara (2015) "Experimental and Theoretical Studies of Volatile Corrosion Inhibitors Adsorption on Zinc Electrode", *Brazilian Chem. Soc.* 26(3): 434-450.
- Tourabi, M., Nohair, K., Nyassi, A., Hammouti, B., Jama, C., Bentiss, F., 2014. Thermodynamic characterization of metal dissolution and inhibitor adsorption processes in mild steel / 3,5-bis(3,4-dimethoxyphenyl)-4-amino-1,2,4-triazole / hydrochloric acid system. *JMES* 5, 1133–1143.
- Walczak, S., Morales-Gil, P., Lindsay, R., 2018. Determining Gibbs energies of adsorption from corrosion inhibition efficiencies: Is it a reliable approach. *Corros. Sci.* 155, 182–185.
- Zarrok, H., Zarrouk, A., Hammouti, B., Salghi, R., Jama, C., Bentiss, F., 2012. Corrosion control of carbon steel in phosphoric acid by purpald–weight loss, electrochemical and XPS studies. *Corros. Sci.* 64, 243–252.
- Zarrouk, A., Zarrok, H., Salghi, R., Bouroumane, N., Hammouti, B., Al-Deyab, S.S., Touzani, R., 2012. The Adsorption and Corrosion Inhibition of 2- [Bis- (3, 5- dimethyl-pyrazol-1-ylmethyl) -amino] -pentanedioic Acid on Carbon Steel Corrosion in 1.0 M HCl. *Int. J. Electrochem. Sci.* 7, 10215–10232.
- Zarrouk, A., Hammouti, B., Dafali, A., Bouachrine, M., Zarrok, H., Boukhris, S., Al-deyab, S.S., 2014. A theoretical study on the inhibition efficiencies of some quinoxalines as corrosion inhibitors of copper in nitric acid. *J. Saudi Chem. Soc* 18 (5), 450–455.